Received: 14 February 2022 | Revised: 15 April 2022 | Accepted: 13 May 2022

DOI: 10.1002/mgg3.1999

Molecular Genetics & Genomic Medicine Open Access WILEY

ORIGINAL ARTICLE

Two novel *AMHR2* gene variants in monozygotic twins with persistent Müllerian duct syndrome: A case report and functional study

Hong Chen | **Peng Lin** | **Xin Yuan** | **Ruimin Chen**

Department of Endocrinology, Genetics and Metabolism, Fuzhou Children's Hospital of Fujian Medical University, Fuzhou, China

Correspondence
Ruimin Chen, Department of Endocrinology, Genetics and Metabolism, Fuzhou Children's Hospital of Fujian Medical University, Fuzhou 350005, China.
Email: chenrm321@sina.com

Funding information
This work was sponsored by grants from the Key Clinical Special Discipline Construction Program of Fuzhou, Fujian, P.R.C (Grant No. 201610191), Clinical medical center (Grant No. 201808310), The Basic and Clinical Research of Rare Disease of Fuzhou, Fujian, P.R.C (No. ZD-2019-01)

Abstract

Background: Persistent Müllerian duct syndrome (PMDS) is an autosomal recessive congenital abnormality in which Müllerian derivatives, uterus, cervix, upper two-thirds of the vagina, and fallopian tubes persist in otherwise normally virilized males. Mutations in anti-Müllerian hormone (*AMH*) and AMH receptor type II (*AMHR2*) genes have been identified as causative. However, functional experimental analysis of AMHR2 or AMH variants that cause PMDS is still lacking.

Materials and Methods: A Chinese Han family affected by PMDS was identified. To assess the history and clinical manifestations of PMDS, physical, operational, ultrasonographical, pathological, and other examinations were performed on family members. The variant screening was conducted using trio whole-exome sequencing (trio WES) and Sanger sequencing. Complementation-based NanoLuciferase Binary Technology (NanoBiT) was used to examine the interaction between AMH and AMHR2 variants in vivo. The effect of the two variants on the transcriptional activity of the TGFβ/BMP pathway was evaluated using a luciferase assay.

Results: Classic phenotypic manifestations of PMDS in a pair of identical twins were described and confirmed by genetic sequence analysis. Molecular studies revealed two novel variants c.118G > C [p.(Gly40Arg)], c.1222G > C [p.(Ala408Pro)] in the *AMHR2* gene. The AMHR2 p.Gly40Arg variant reduces its ability to bind to AMH, while the p.Ala408Pro variant alters the kinase domain structure. Both variants significantly reduce TGFβ/BMP signaling.

Conclusion: Two missense AMHR2 variants associated with PMDS were identified. These findings provide novel insights toward better clinical evaluation and further understanding of the molecular basis of PMDS.

KEYWORDS

AMH, *AMHR2* gene, persistent Müllerian duct syndrome, variants

[Correction added on July 13, 2022 after first online publication. The figure 3 has been corrected in this version.]

1 | INTRODUCTION

Persistent Müllerian duct syndrome (PMDS) is a rare autosomal recessive inherited disorder of internal male sexual development, characterized by impaired regression of Müllerian ducts. To date, approximately 200 patients with PMDS have been reported since the initial description of this disease by Nilson (Farikullah et al., 2012).

Newborn male twins had a 46, XY karyotype with external male genitalia, and the urethra meatus was at the tip of the penis (no hypospadias) (Unal et al., 2021). However, both had internal Müllerian duct structures, including a uterus, cervix, fallopian tubes, and upper two-thirds of the vagina. Approximately 45% of cases are caused by absolute or relative deficiencies of an anti-Müllerian hormone (AMH), 40% by AMH receptor type II (AMHR2), and in 15% of cases, the etiology is unknown (Pulido et al., 2017). In the male embryo, Müllerian structures regress under the effect of AMH around the seventh week of gestation, releasing the testes from their initial positions in the pelvis to descend to the scrotum, provided the cord length is sufficient. If Müllerian ducts fail to regress, the testes remain suspended in the broad ligament. PMDS is usually diagnosed during orchidopexy or inguinal herniorrhaphy (Pulido et al., 2017).

Herein, we describe the clinical characteristics of a pair of monozygotic twins with PMDS. Gene sequencing revealed two missense variants, c.118G > C [p.Gly40Arg)] and c.1222G > C [p.Ala408Pro)], in the *AMHR2* gene. A series of functional assays were performed to elucidate the pathogenic mechanisms underlying *AMHR2* variants.

2 | METHODS

2.1 | Study subjects

This study was reviewed and approved by the Ethics Committee of Fuzhou Children's Hospital of Fujian Medical University and was conducted in agreement with the Declaration of Helsinki (No. 201921). The twins were born to unrelated Chinese parents of Han ethnicity. Written informed consent was obtained from the parents.

2.2 | Targeted next-generation sequencing and data analysis

Peripheral venous blood (5 ml) was collected from the twins and their parents for gene analysis. The extracted DNA was fragmented with DNAase, followed by polymerase chain reaction (PCR) amplification and ligation of the linker sequence. The DNA sample was purified twice using the TruSight One Sequencing Panel (Illumina Inc, USA), and then further amplified and purified by PCR. The final library was sequenced on a MiSeq sequencer (Illumina Inc, USA), and the exon region of 4811 was analyzed for clinically relevant genes. PMDS-related genes were finally sequenced (http://www.illumina.com/).

All data were aligned to the human reference sequence (UCSC hg19) using the BWA algorithm. All clinical data were analyzed using bioinformatics software. The function, variation, and genetic pattern of each gene were inspected for candidate variants. The Sanger sequencing variant detected in the *AMHR2* gene was described according to the NCBI entry NG_015981.1 (NM_020547.3). The variants were named according to the Human Genome Variation Society (HGVS) sequence variant nomenclature.

2.3 | Conservative and pathogenicity analysis of the variant

AMHR2 protein sequences were downloaded from the Uniprot database (https://www.uniprot.org/) and the ClustalX program (http://ftp-igbmc.u-strasbg.fr/pub/ClustalX/) was used for sequence alignment. Sequence alignment results were displayed online using ConSurf (https://consurf.tau.ac.il/) (Ashkenazy et al., 2016). The variants' pathogenicity was analyzed using the webserver PREDICT-SNP (https://loschmidt.chemi.muni.cz/predictsnp1/) (Bendl et al., 2014).

2.4 | Three-dimensional (3D) structure modeling

The amino acid sequence of wild-type human AMHR2 was retrieved from the UniProt database (http://www.uniprot.org). The Three-dimensional structure of the wild-type human AHMR2 was generated using SWISS-MODEL (https://swissmodel.expasy.org/) (Studer et al., 2020; Waterhouse et al., 2018). The online server Dynamut (http://biosig.unimelb.edu.au/dynamut/) was used to assess the local conformation of wild-type and variant proteins (Rodrigues et al., 2018). The structural representation was generated using the molecular visualization system in the open-source foundation PyMOL 2.4 (https://pymol.org/2/).

2.5 | Analysis of the interaction between AMHR2 and AMH

NanoLuc® Binary Technology (NanoBiT) (Promega, Cat#N2014), a structural complementation reporter system, was used to analyze protein interactions. NanoBiT consists of a Large BiT (LgBiT; 18 kDa) subunit and a

small complementary peptide (SmBiT; 3.6 kDa) (Dixon et al., 2016). When the two target proteins interact, the LgBiT and SmBiT subunits converge to form an active enzyme and produce a bright luminescent signal in the presence of a substrate. The primers used for plasmid construction are listed in Table S1. For NanoBiT protein interaction experiments, *AMHR2* gene coding sequences, and the N-terminus of the SmBiT were fused to form the AMHR2-SmBiT-N plasmid. The *AMH* gene and the C-terminus of LgBiT were fused to form the AMH-LgBiT-C expression plasmid. The wild-type full-length human *AMHR2* (NM_001164690) and *AMH* (NM_000479) complementary DNA (cDNA) were chemically synthesized. HEK293T cells were co-transfected with AMHR2-SmBiT-N and AMH-LgBiT-C to assess the ability of the wild-type, p.Gly40Arg, and p.Ala408Pro of AMHR2 to interact with AMH. The cells were then transfected using jetOPTIMUS® in vitro DNA transfection reagent (Polyplus, Cat#117–07). The DNA ratio was 1:1 when each different variant was co-transfected. After 24 h of transfection, the culture medium was replaced with fresh Opti-MEM (Cat# 51985091), and 100 µl diluted substrate was added directly to 96-well plates. Transfection efficiency was determined using quantitative real-time PCR (qPCR). Primers used for qPCR are listed in Table S2. The fluorescence intensity was measured with a VICTOR Nivo multimode plate reader (Thermo Fisher, ND-1000). The experiments were repeated independently at least three times in triplicate. Data are expressed as mean ± standard deviation (*SD*) and analyzed using a Mann–Whitney *U* test.

2.6 | TGF-β/BMP luciferase assay

For transient transfection, HEK-293 T cells were transfected using jetOPTIMUS® in vitro DNA transfection reagent. HEK-293 T cells were co-transfected with the AMH expression vector, pGL3 BRE Luciferase wild-type, or variants of AMHR2 expression vectors. The DNA ratio of *AMHR2*, *AMH*, and flash reporter plasmids was 2:2:1 when each different variant was co-transfected (Hart et al., 2021; Malone et al., 2019). The luciferase reporter assay system (Promega, USA) was used 48 h after transfection. The experiments were repeated independently at least seven times in triplicates. Data are expressed as mean ± *SD* and analyzed using a Mann–Whitney *U* test.

2.7 | Western blotting and qPCR

The western blotting and qPCR analyses were conducted as previously described (Chen et al., 2019). Information on the primers is presented in Table S2.

2.8 | Cell culture

Cell cultures were prepared and maintained according to standard cell culture procedures. HEK293T cells were cultured in high glucose Dulbecco's modified Eagle's medium (HG-DMEM) (Invitrogen, USA) containing 10% fetal bovine serum (Gibco, USA). Cells were grown at 37°C with 5% CO_2.

2.9 | Statistical analysis

Statistical analyses were performed using the GraphPad Prism 7 program. Statistical significance was analyzed using a Mann–Whitney *U* test. All results were confirmed by at least three independent experiments. Data are represented as mean ± *SD* ($n \geq 3$). $^{*}p < .05$, $^{**}p < .01$, and $^{***}p < .001$.

3 | RESULTS

3.1 | Clinical evaluation

3.1.1 | Case one

A monozygotic 20-month-old Chinese male was referred to the pediatric surgery department of Fuzhou Children's Hospital of Fujian Medical University due to a left inguinal hernia and impalpable right testis. His height (85.2 cm) and weight (9.8 kg) were normal with male external genitalia and a penile length of 4.5 cm (normal for age on a penile curve). The urethral opening was at the tip of the penis. The right testicle was not palpable in the scrotum or inguinal region. A left inguinal hernia was present. Ultrasonic examination detected a left testis in the groin and suspicious testis in the right iliac fossa on sonography. His serum AMH level was normal (112 ng/ml; normal range 74.1–148.1 ng/ml). Other relevant biochemical data are displayed in Table 1. Cytogenetic studies in 50 metaphases revealed a 46, XY karyotype. Two weeks later, he underwent laparoscopic examination of the gonad, high ligation of the hernia sac, and reduction of the testis. An ovarian-like tissue, fallopian tubes, and 1.5 × 0.8 cm uterus were found intra-operative, but no apparent right testis was found. The left inguinal hernia was repaired and an ovarian-like tissue, fallopian tubes, and uterus were extirpated. Pathological examination showed that the gonadal tissue was an immature testicle with immature Leydig and Sertoli cells. The postoperative diagnosis was PMDS.

TABLE 1 Clinical data of the monozygotic twins

Items	Patients		
	Twin one (II-1)	**Twin two (II-2)**	
Age at initial diagnosis	20-month-old	20-month-old	
Chromosome karyotype	46, XY	46, XY	
Genitalia phenotype	Impalpable right testis, left inguinal hernia	Bilateral cryptorchidism, transverse testicular ectopia	
Blood hormonal characteristics			**Normal value**
FSH	0.16	0.13	0.00–5.50 IU/L
LH	0.77	0.80	0.00–4.10 IU/L
DHT	17.34	85.96	pg/ml
Androstenedione	<0.3	<0.3	0.7–3.6 ng/ml
DHEA-S	<15	<15	80–560 μg/dl
Testosterone	2.5	2.5	ng/ml
Testosterone of post-hCG level	–	373.7	ng/ml
AMH	108.0	112.0	74.1–148.1 ng/ml
Inhibin B	163.85	139.48	33.78–339.64 pg/ml

Abbreviations: AMH, anti-Müllerian hormone; DHEA-S, dehydroepiandrosterone sulfate; FSH, follicle-stimulating hormone; hCG, human chorionic gonadotropin; LH, luteinizing hormone.

3.1.2 | Case two

Considering that his twin was diagnosed with PMDS, he was subsequently examined in our hospital. Physical examination of the patient revealed male external genitalia with an empty scrotum, no palpable testes, and a penile length of 5 cm (normal for age). The urethral opening was at the tip of the penis. A 1.0×0.8 cm mass was present in the right inguinal region, and the left testis was not found in the inguinal area. Ultrasound examination revealed both testes of standard size in the right inguinal canal. Serum AMH level was normal (108 ng/ml). Other relevant biochemical data are displayed in Table 1. Chromosomal analysis showed a 46, XY karyotype. The prostate could be detected by sonography. During exploratory surgery, bilateral testes were found in the right groin, and a uterus and bilateral fallopian tubes were found in the pelvic cavity. The postoperative diagnosis was PMDS. Detailed clinical characteristics of the monozygotic twins are presented in Table 1.

3.2 | Genetic diagnosis

Mutational analysis of the *AMHR2* gene identified pathogenic mutations in the monozygotic twins, confirming the diagnosis of PMDS. Two novel variants, c.118G>C [p.(Gly40Arg)] and c.1222G>C [p.(Ala408Pro)], of the *AMHR2* gene (OMIM * 600957) were identified. The father carried the heterozygous mutation c.1222G>C [p.(Ala408Pro)], whereas the mother carried the heterozygous mutation c.118G>C [p.(Gly40Arg)] (Figure 1a,b). The missense variants were absent from the public population database gnomAD (http://gnomad), Chinese Millionome Database (http://cmdb.bgi.com/), and Human Gene Mutation Database (HGMD, http://www.hgmd.org/). According to the American College of Medical Genetics and Genomics (ACMG) criteria, both p.Gly40Arg and p.Ala408Pro were likely pathogenic variants (Richards et al., 2015).

To further elucidate the genetic test results, the interspecific conservation and pathogenicity of this variant were analyzed. AMHR2 protein sequences in 13 mammals were compared, including *Homo sapiens*, *Pan troglodytes*, *Macaca mulatta*, *Myotis lucifugus*, *Equus caballus*, *Ailuropoda melanoleuca*, *Felis catus*, *Canis lupus familiaris*, *Bos taurus*, *Sus scrofa*, *Oryctolagus cuniculus*, *Loxodonta africana*, and *Mus musculus*. The residues at positions 40 and 408 of AMHR2 were highly conserved across these representative mammals (Figure 1c). Both missense variants of *AMHR2* were predicted to be deleterious for all six predictors (PredictSNP, MAPP, PhD-SNP, PolyPhen1, PolyPhen2, and SIFT), indicating a deleterious effect of both variants with a high confidence score (Table 2). Hence, c.118G>C [p.(Gly40Arg) and c.1222G>C [p.(Ala408Pro)] variants in *AMHR2* are almost certainly pathogenic.

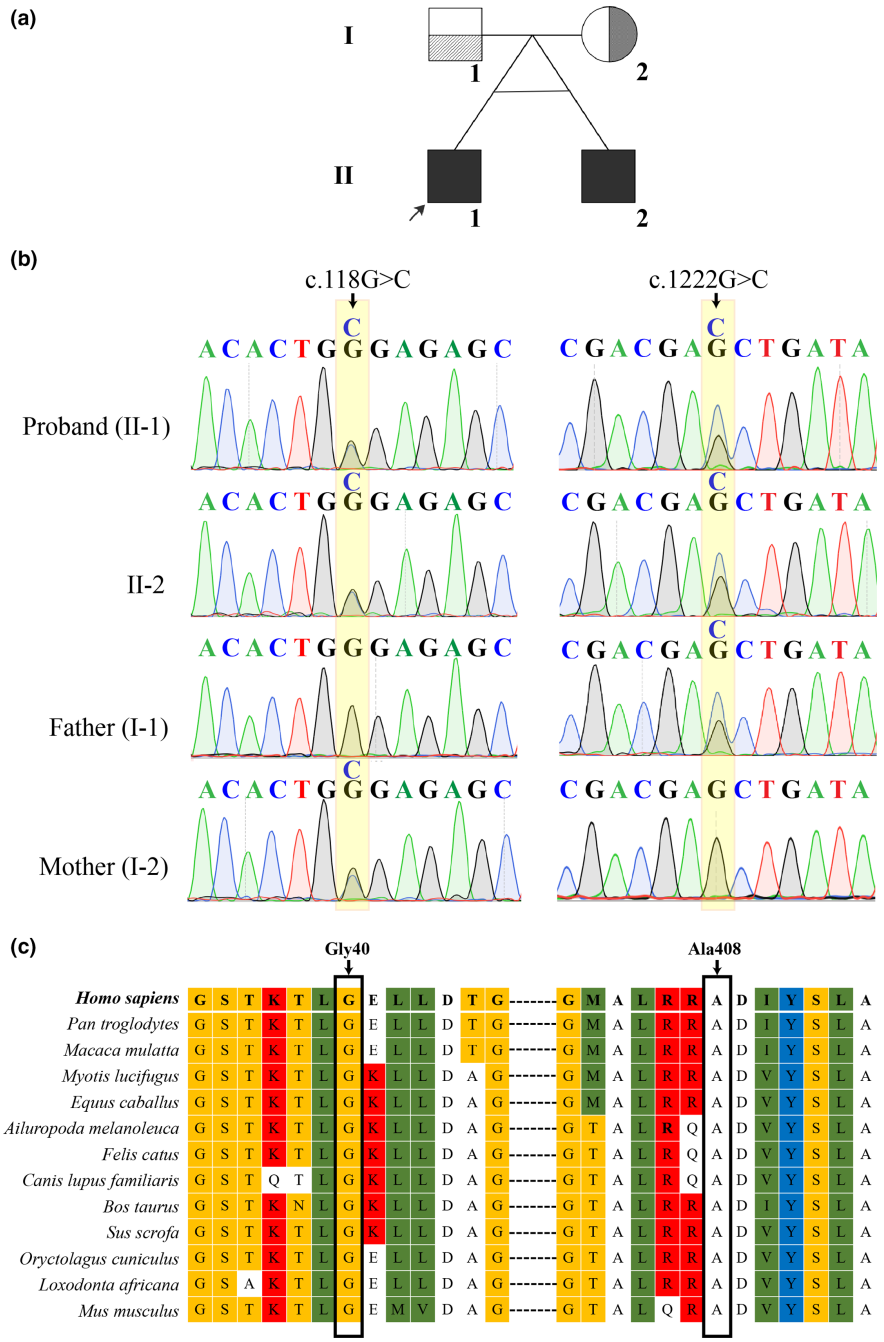

FIGURE 1 *AMHR2* gene variants in the twins and their family members. (a) Pedigree of the family with PMDS. Squares represent males and circles represent females. The proband is indicated by an arrow. Affected individuals are shown as filled black symbols and half-filled symbol is clinically unaffected subjects harboring a heterozygous variant. (b) Sanger sequencing chromatograms showing that the twins carry compound heterozygous variants, c.118G > C [p.(Gly40Arg)] and c.1222G > C [p.(Ala408Pro)], in the *AMHR2* gene. Mother (I-2) has a heterozygous c.118G > C variant and the father (I-1) carries the heterozygous c.1222G > C variant. (c) A conservative analysis across diverse mammals.

TABLE 2 Predictions and confidence scores for AMHR2 variants obtained with the PREDICT-SNP server

Variants	p.Gly40Arg (prediction; expected accuracy)	p.Ala408Pro (prediction; expected accuracy)
PredictSNP	Deleterious; 72%	Deleterious; 87%
MAPP	Deleterious; 46%	Deleterious; 77%
PHD-SNP	Deleterious; 58%	Deleterious; 82%
PolyPhen-1	Deleterious; 74%	Deleterious; 74%
PolyPhen-2	Deleterious; 81%	Deleterious; 63%
SIFT	Deleterious; 53%	Deleterious; 43%

3.3 | 3D structure modeling

To further examine the structural changes in AMHR2, the SWISS-MODEL online software was used to conduct protein structure modeling (Figure 2a,d). The DynaMut webserver was used to analyze and visualize protein dynamics and assess the impact of these variants. The DynaMut web server was also used to assess local interactions between wild-type and variant amino acid residues. Given the change difference between glycine (Gly) and Arginine (Arg), the Gly40Arg variant introduces an aberrant change leading to the repulsion of ligands or other residues with a similar charge. The torsion angles at Gly40 for this residue are deviant insofar as only glycine is flexible enough to create these torsion angles. The arginine residue compels the local backbone into an abnormal conformation and disturbs the local structure (Figure 2b,c). The p.Ala408Pro variant causes a significant difference between alanine (Ala) and proline (Pro). In addition, position 408 of the amino acid sequence of AMHR2 is located within the protein kinase domain, substitution of Ala408 by a proline, known to break α-helices, possibly hinders this functional domain. Also, proline causes the loss of hydrogen bonding and introduces hydrophobic bonds, which may interfere with the correct folding of the protein (Figure 2e,f).

3.4 | Affinity between AMHR2 variants and AMH

A luciferase-based protein fragment complementation assay (NanoBiT) was employed to characterize the interaction between AMHR2 and AMH. A clear luminescent signal was obtained when SmBit-AMHR2-N and LgBit-AMH-C were co-expressed, indicating a strong interaction between them (Figure 3a,b). Relative *AMHR2* mRNA expression levels were analyzed 24 h post-transduction using qPCR. No difference was found in *AMHR2* levels (Figure S1). The data are shown in relative luminescence units (RLU). The wild-type values were set at an arbitrary mean value of 1, and the fold change in the mutant group was calculated based on the wild-type group. As shown in Figure 3c, the binding ability of the p.Gly40Arg variant of AMHR2 to AMH was significantly decreased to 32.3%–49.2% of the wild-type. As expected, the p.Ala408Pro variant did not impact the affinity for AMH.

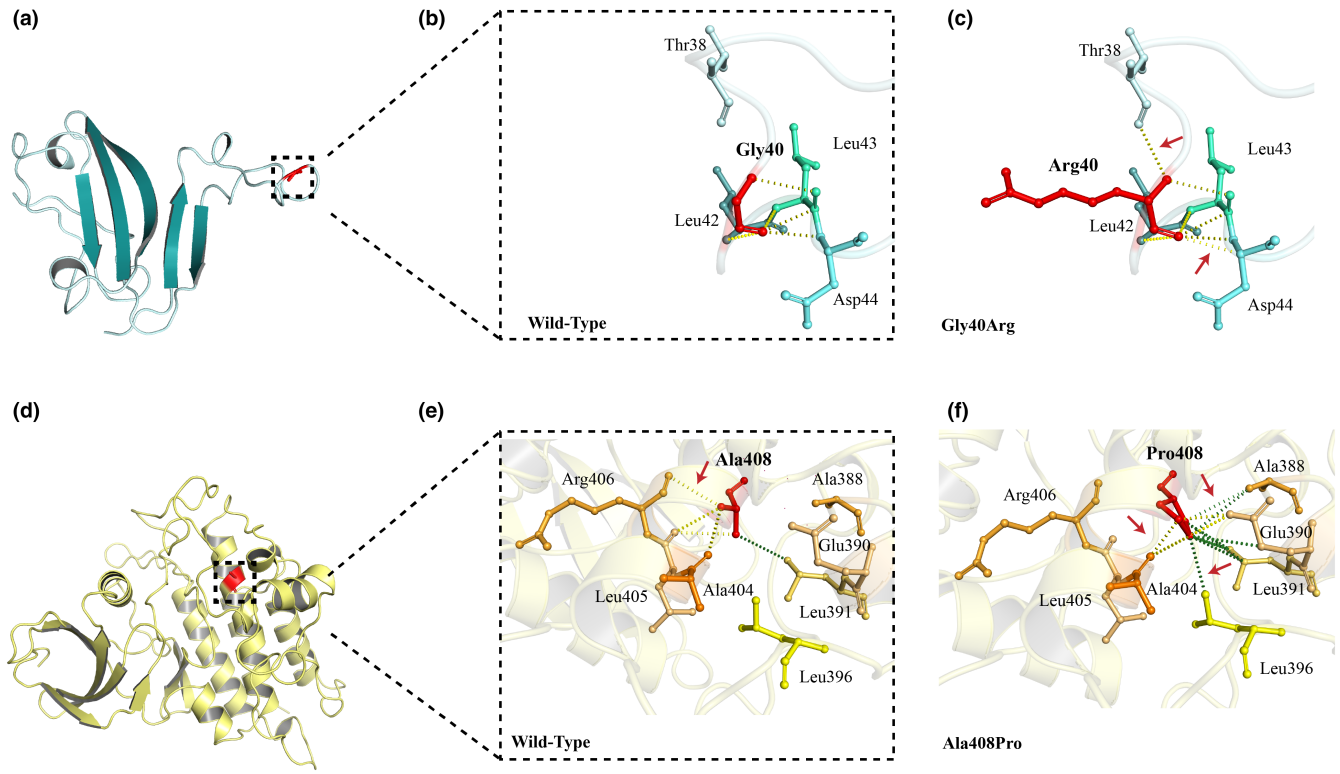

FIGURE 2 Prediction of interactions between amino acid residues. (a) Extracellular structure of the AMHR2 protein. (b) Local structure of the wild-type AMHR2 protein. (c) Local structure of the AMHR2 p.Gly40Arg variant. (d) Schematic diagram of the intracellular AMHR2 structure. (e) Local structure of the wild-type AMHR2 protein. (f) Local structure of the AMHR2 p.Ala408Pro variant. Wild-type and variant residues are colored in red and are also represented as sticks alongside the surrounding residues, which are involved in other types of interactions. The red arrows mark interactions between the altered amino acids and the black arrows point to wild-type or variant amino acid residues. Hydrogen bonding is shown in yellow dotted lines. Hydrophobic bonds are indicated by green dotted lines.

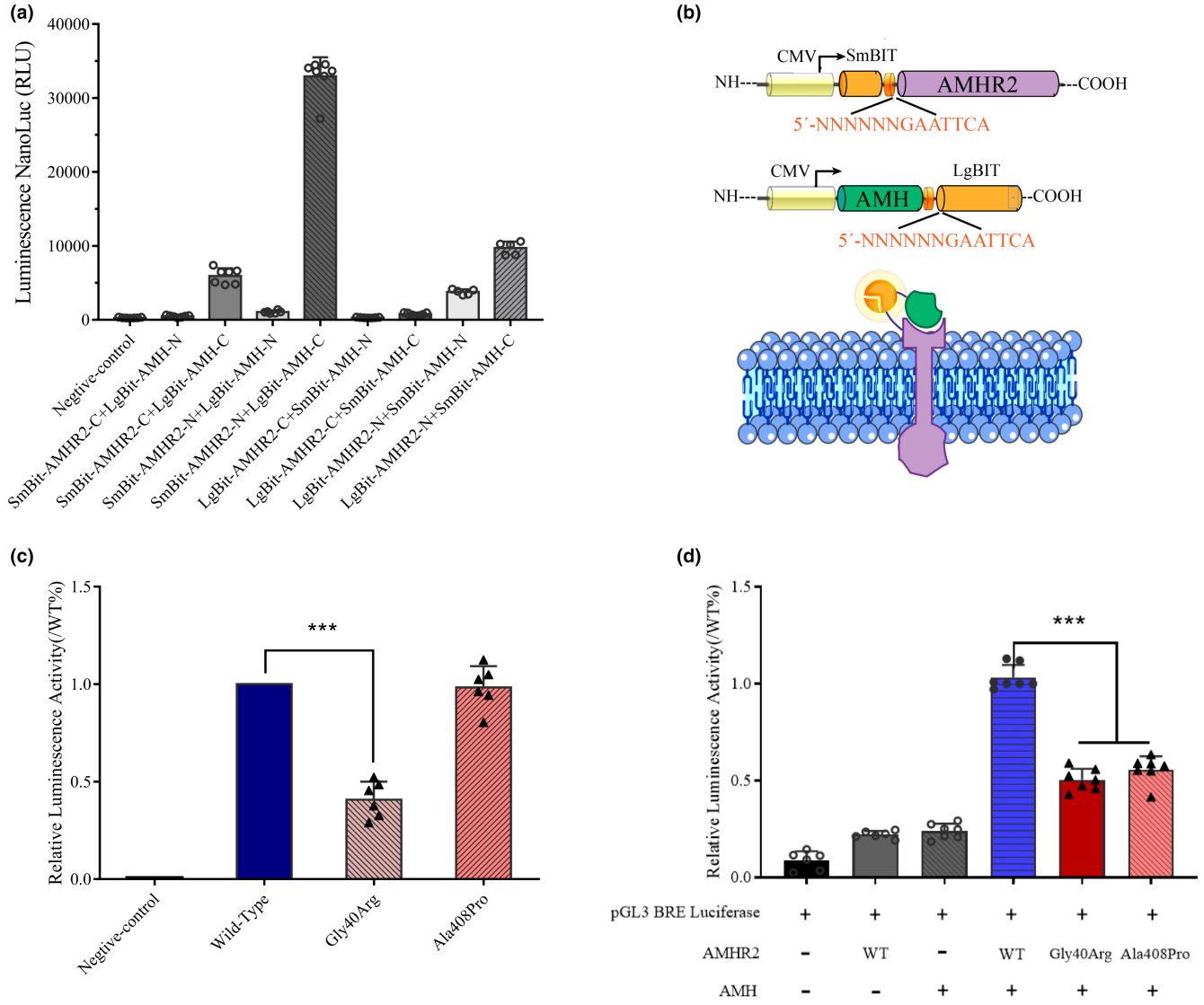

FIGURE 3 Functional analysis of AMHR2 variants. (a–c) Interaction between AMHR2 variants and AMH. (a) HEK293 cells were transiently transfected with eight different combinations of LgBit and SmBit fusion proteins to screen the fusion protein combinations for maximum response. (b) *AMHR2* gene and the N-terminus of the SmBit were fused to form the AMHR2-SmBiT-N plasmid. The *AMH* gene and the C-terminus of LgBit were fused to form the AMH-LgBit-C expression plasmid. Schematic structure of the AMHR2 and AMH NanoBit-fused proteins. (c) After 24 h of co-transfection, the diluted substrate was directly added to each well to measure the absolute value of the NanoBit activity for 30 min. Wild-type values were adjusted to 1′ for comparison, and the relative value of AMHR2-AMH binding capacity is represented by a histogram. (d) HEK293T cells were co-transfected with wild-type or AMHR2 variants expression plasmids and TGF-β/BMP flash reporter plasmids. The plus (+) and minus (−) signs below the x-axis indicate whether pGL3 BRE luciferase plasmids and AMHR2 and AMH expression plasmids have been added, respectively. Wild-type values were adjusted to 1′ for comparison, and the relative value of transcriptional activities is represented by a histogram. Each value represents the mean ± *SD* from at least three independent cultures (***$p < .001$ by Mann–Whitney *U* test).

3.5 | TGF-β/BMP luciferase assay

To determine the effect of the variant on the AMH/AMHR2 signal pathway, the transcriptional activity of TGF-β/BMP was evaluated by pGL3 BRE Luciferase (plasmid 45,126; Addgene). As expected, the luciferase activity, as driven by the pGL3 BRE Luciferase transcriptional response elements, increased significantly when HEK-293 T cells were transfected with BRE promoter flash reporter plasmids and wild-type or variant expression vectors (especially in the wild-type group). The data are shown in RLU (Figure 3d). The wild-type values were designated at an arbitrary mean value of 1, and the fold change in the mutant group was calculated according to the wild-type group. At 48 h after transfection, the p.Gly40Arg or p.Ala408Pro variant significantly diminished the signaling

pathway of AMH/AMHR2 to 33.4% and 38.9% of the wild-type, respectively. No difference in protein expression was found between wild-type and mutant AMHR2 (Figure S2).

4 | DISCUSSION

PMDS is a sui generis inherited disorder of sexual differentiation characterized by failure of regression of Müllerian ducts in XY males (Unal et al., 2021). A Chinese family with this rare disorder and pathogenic mutations in *AMHR2* was studied. Compound heterozygous mutations were uncovered in monozygotic twins. The clinical phenotype of *AMH* and *AMHR2* mutations are characteristically indistinguishable (Hutson et al., 2014). Typically, a male reproductive tract and a male phenotype are present with inconspicuous fallopian tubes and uterine structures. Approximately 55% of patients have bilateral cryptorchidism, 20% have unilateral cryptorchidism and/or contralateral hernia, and a small proportion of patients have a uterine inguinal hernia. Before 9 months of age, reducing the testis may prevent deterioration of reproductive function (Mazen et al., 2017). Transverse testicular ectopia (TTE) is an uncommon congenital male reproductive dysplasia in which both testicles are found in the same inguinal canal (Barrack, 1994; Yu et al., 2020). Approximately 25%–30% of patients with PMDS also have TTE (Kaul et al., 2011; Picard et al., 2017; Shalaby et al., 2014). TTE is associated with PMDS, yet the role of AMH in the process of testicular descent is unclear, but it is possibly related to gubernaculum testis function (Alp et al., 2014). Recent studies have shown that AMH may shorten the gubernendar line in humans (Hutson & Lopez-Marambio, 2017). It is plausible that the irregular adhesion between the fetal testis and Müllerian remnants begets TTE. Weiss et al. (Weiss et al., 1978) reported a pair of PMDS twins with identical clinical phenotypes. However, monozygotic PMDS twins in the current study had the same genotype but different phenotypes. One had an inguinal hernia and unilateral cryptorchidism, and the other had TTE. The genotype of *AMH* and *AMHR2* genes are independent of the phenotype (Altincik et al., 2017; Hutson et al., 2014; Mazen et al., 2011; Morikawa et al., 2014; van der Zwan et al., 2012). Environmental or other genetic factors may lead to discordant phenotypes despite identical genotypes, but the specific mechanism is unclear. Given that the testes are the sole source of AMH, serum AMH levels reflect functional Sertoli cells. Serum AMH is depressed in patients with *AMH* gene variants, whereas high or average concentrations are typical of *AMHR2* variants. Thus, normal AMH levels usually exclude AMH synthesis mutations. AMH variant p.(Gln496His) hinders ligand binding (Belville et al., 2004). Normal serum AMH is not necessarily an *AMHR2* gene variant because a genetic cause is not identified in 15% of patients. PMDS diagnosis requires differentiation from dysgenetic male pseudohermaphroditism and mixed gonadal dysgenesis. The dysgenetic male pseudohermaphroditism results from the complete failure of both testes. With the persistence of Müllerian duct structures and the ambiguity of external genitalia, mixed gonadal dysgenesis is characterized by a contralateral streak gonad, typically in the setting of 45, X/46, XY or 46, XY karyotype. Müllerian duct structures are preserved along with the ambiguity of external genitalia.

AMHR2 gene is located in 12q13, including 11 exons, encoding three functional receptor areas: the extracellular domain (exon 1–3), a single transmembrane hydrophobic region (exon 4), and an intracellular serine/threonine kinase domain (exon 5–11). According to the HGMD Professional 2020.4, about 103 different deleterious *AMHR2* gene variants have been identified, which give rise to PMDS. The kinase domain (amino acid 203–518) plays a vital role in identifying the substrate. Position 408 of the amino acid sequence of AMHR2 is located within the protein kinase domain and substitution of Ala408 by a proline, known to break α-helices, could disrupt interference with this domain and affect the correct folding of the protein. In our case, the AMHR2 p.Ala408Pro variant affects a functional domain, resulting in impaired substrate recognition and affinity. For the p.Gly40Arg variant, the arginine residue disfigures the local backbone and alters function. The unique structural disturbance of the p.Gly40Arg variant modifies the local hydrogen bond pattern of AMHR2, resulting in decreased variant flexibility. Known protein–protein interactions require the flexibility of local domains to ensure protein function and activity (Jarosch, 2005; Pauwels & Tompa, 2016). That is to say, the Gly40Arg variant deforms the structure of the extracellular domain and hampers ligand binding. The effect of the binding ability of AMHR2 variants to its ligand AMH was evaluated using a luciferase-based protein fragment complementation assay. The results revealed that the binding ability of the p.Gly40Arg variant to AMH was profoundly reduced. As mentioned earlier, the flexibility of the extracellular domain of the AMHR2 mutant protein is compromised, which may disrupt AMH binding. Finally, the TGF-β/BMP luciferase assay demonstrated that both variants partially attenuated the transduction of the AMH/AMHR2 signaling pathway. The change in the AMH binding ability of AMHR2 variants was assessed using a new approach, and the pathogenicity of both variants identified in our twins was demonstrated.

5 | CONCLUSIONS

In summary, the present study presents a monozygotic twin pair with PMDS with two novel variants in the *AMHR2* gene. The results showed that the AMHR2 p.Gly40Arg variant had a reduced ability to bind to AMH, while p.Ala408Pro variant undermines the function of the kinase domain, both of which synergistically diminish AMH/AMHR2 signaling. These findings provide insights into the clinical evaluations and molecular basis of PMDS.

AUTHOR CONTRIBUTIONS

Hong Chen: Writing-Original Draft, Investigation, and Validation; **Peng Lin**: Data curation. **Ruimin Chen**: Conceptualization, Methodology, Writing-Review & Editing; **Xin Yuan**: Writing-Review.

ACKNOWLEDGMENTS

The authors are grateful to the family members and patients for their participation in this study.

CONFLICT OF INTEREST

There are no competing financial or nonfinancial interests.

DATA AVAILABILITY STATEMENT

All datasets generated for this study are included in the article.

ETHICS APPROVAL AND CONSENT TO PARTICIPATE

This study was reviewed and approved by the Ethics Committee of Fuzhou Children's Hospital of Fujian Medical University and was conducted in agreement with the Declaration of Helsinki.

CONSENT FOR PUBLICATION

All authors consent for publication.

ORCID

Ruimin Chen https://orcid.org/0000-0003-4114-7706

REFERENCES

Alp, B. F., Demirer, Z., Gürağaç, A., Babacan, O., Sarı, E., Sarı, S., & Yavan, I. (2014). Persistent Mullerian duct syndrome with transverse testicular ectopia and seminoma. *International Urology and Nephrology*, *46*(8), 1557–1562. https://doi.org/10.1007/s11255-014-0667-4

Altincik, A., Karaca, F., & Onay, H. (2017). Persistent Müllerian duct syndrome: A novel mutation in the *A*nti-Müllerian *H*ormone gene. *Hormones (Athens, Greece)*, *16*(2), 205–208. https://doi.org/10.14310/horm.2002.1735

Ashkenazy, H., Abadi, S., Martz, E., Chay, O., Mayrose, I., Pupko, T., & Ben-Tal, N. (2016). ConSurf 2016: An improved methodology to estimate and visualize evolutionary conservation in macromolecules. *Nucleic Acids Research*, *44*(W1), W344–W350. https://doi.org/10.1093/nar/gkw408

Barrack, S. (1994). Crossed testicular ectopia with fused bilateral duplication of the vasa deferential: An unusual finding in cryptochidism. *East African Medical Journal*, *71*(6), 398–400.

Belville, C., Van Vlijmen, H., Ehrenfels, C., Pepinsky, B., Rezaie, A. R., Picard, J.-Y., Josso, N., Clemente, N. D., & Cate, R. L. (2004). Mutations of the anti-mullerian hormone gene in patients with persistent mullerian duct syndrome: Biosynthesis, secretion, and processing of the abnormal proteins and analysis using a three-dimensional model. *Molecular Endocrinology (Baltimore Md.)*, *18*(3), 708–721.

Bendl, J., Stourac, J., Salanda, O., Pavelka, A., Wieben, E. D., Zendulka, J., Brezovsky, J., & Damborsky, J. (2014). PredictSNP: Robust and accurate consensus classifier for prediction of disease-related mutations. *PLoS Computational Biology*, *10*(1), e1003440. https://doi.org/10.1371/journal.pcbi.1003440

Chen, H., Yuan, K., Zhang, B., Jia, Z., Chen, C., Zhu, Y., Sun, Y., Zhou, H., Huang, W., Liang, L., Yan, Q., & Wang, C. (2019). A novel compound heterozygous variant causes 17α-hydroxylase/17, 20-lyase deficiency. *Frontiers in Genetics*, *10*, 996. https://doi.org/10.3389/fgene.2019.00996

Dixon, A. S., Schwinn, M. K., Hall, M. P., Zimmerman, K., Otto, P., Lubben, T. H., Butler, B. L., Binkowski, B. F., Machleidt, T., Kirkland, T. A., Wood, M. G., Eggers, C. T., Encell, L. P., & Wood, K. V. (2016). NanoLuc complementation reporter optimized for accurate measurement of protein interactions in cells. *ACS Chemical Biology*, *11*(2), 400–408. https://doi.org/10.1021/acschembio.5b00753

Farikullah, J., Ehtisham, S., Nappo, S., Patel, L., & Hennayake, S. (2012). Persistent Müllerian duct syndrome: Lessons learned from managing a series of eight patients over a 10-year period and review of literature regarding malignant risk from the Müllerian remnants. *BJU International*, *110*(11 Pt C), E1084–E1089. https://doi.org/10.1111/j.1464-410X.2012.11184.x

Hart, K. N., Stocker, W. A., Nagykery, N. G., Walton, K. L., Harrison, C. A., Donahoe, P. K., Pépin, D., & Thompson, T. B. (2021). Structure of AMH bound to AMHR2 provides insight into a unique signaling pair in the TGF-β family. *Proceedings of the National Academy of Sciences of the United States of America*, *118*(26), e2104809118. https://doi.org/10.1073/pnas.2104809118

Hutson, J. M., Grover, S. R., O'Connell, M., & Pennell, S. D. (2014). Malformation syndromes associated with disorders of sex development. *Nature Reviews Endocrinology*, *10*(8), 476–487. https://doi.org/10.1038/nrendo.2014.83

Hutson, J. M., & Lopez-Marambio, F. A. (2017). The possible role of AMH in shortening the gubernacular cord in testicular descent: A reappraisal of the evidence. *Journal of Pediatric Surgery*, *52*(10), 1656–1660. https://doi.org/10.1016/j.jpedsurg.2017.05.021

Jarosch, R. (2005). The alpha-helix, an overlooked molecular motor. *Protoplasma*, *227*(1), 37–46.

Kaul, A., Srivastava, K. N., Rehman, S. M. F., Goel, V., & Yadav, V. (2011). Persistent Müllerian duct syndrome with transverse testicular ectopia presenting as an incarcerated inguinal hernia. *Hernia: The Journal of Hernias and Abdominal Wall Surgery*, *15*(6), 701–704. https://doi.org/10.1007/s10029-010-0707-7

Malone, S. A., Papadakis, G. E., Messina, A., Mimouni, N. E. H., Trova, S., Imbernon, M., Allet, C., Cimino, I., Acierno, J., Cassatella, D., Xu, C., Quinton, R., Szinnai, G., Pigny, P., Alonso-Cotchico, L., Masgrau, L., Maréchal, J. D., Prevot, V., Pitteloud, N., & Giacobini, P. (2019). Defective AMH signaling disrupts GnRH neuron development and function and contributes to hypogonadotropic hypogonadism. *eLife*, *8*, e47198. https://doi.org/10.7554/eLife.47198

Mazen, I., Abdel Hamid, M. S., El-Gammal, M., Aref, A., & Amr, K. (2011). AMH gene mutations in two Egyptian families with persistent müllerian duct syndrome. *Sexual Development*, *5*(6), 277–280. https://doi.org/10.1159/000334854

Mazen, I., El-Gammal, M., McElreavey, K., Elaidy, A., & Abdel-Hamid, M. S. (2017). Novel AMH and AMHR2 mutations in two Egyptian families with persistent Müllerian duct syndrome. *Sexual Development*, *11*(1), 29–33. https://doi.org/10.1159/000455019

Morikawa, S., Moriya, K., Ishizu, K., & Tajima, T. (2014). Two heterozygous mutations of the AMH gene in a Japanese patient with persistent Müllerian duct syndrome. *Journal of pediatric Endocrinology & Metabolism: JPEM*, *27*(11–12), 1223–1226. https://doi.org/10.1515/jpem-2014-0111

Pauwels, K., & Tompa, P. (2016). Editorial: Function and flexibility: Friend or foe? *Frontiers in Molecular Biosciences*, *3*, 31. https://doi.org/10.3389/fmolb.2016.00031

Picard, J.-Y., Cate, R. L., Racine, C., & Josso, N. (2017). The persistent Müllerian duct syndrome: An update based upon a personal experience of 157 cases. *Sexual Development*, *11*(3), 109–125. https://doi.org/10.1159/000475516

Pulido, L., Iwasiuk, G., Sparkuhl, M., Bui, D., & Springs, H. (2017). Persistent Mullerian duct syndrome presenting in an incarcerated recurrent inguinal hernia with hydrocele. *Urology Case Reports*, *12*, 47–48. https://doi.org/10.1016/j.eucr.2017.02.007

Richards, S., Aziz, N., Bale, S., Bick, D., Das, S., Gastier-Foster, J., Grody, W. W., Hegde, M., Lyon, E., Spector, E., Voelkerding, K., Rehm, H. L., & ACMG Laboratory Quality Assurance Committee. (2015). Standards and guidelines for the interpretation of sequence variants: A joint consensus recommendation of the American College of Medical Genetics and Genomics and the Association for Molecular Pathology. *Genetics in Medicine*, *17*(5), 405–424. https://doi.org/10.1038/gim.2015.30

Rodrigues, C. H., Pires, D. E., & Ascher, D. B. (2018). DynaMut: Predicting the impact of mutations on protein conformation, flexibility and stability. *Nucleic Acids Research*, *46*(W1), W350–W355. https://doi.org/10.1093/nar/gky300

Shalaby, M. M., Kurkar, A., Zarzour, M. A., Faddan, A. A., Khalil, M., & Abdelhafez, M. F. (2014). The management of the persistent Müllerian duct syndrome. *Arab Journal of Urology*, *12*(3), 239–244. https://doi.org/10.1016/j.aju.2014.04.001

Studer, G., Rempfer, C., Waterhouse, A. M., Gumienny, R., Haas, J., & Schwede, T. (2020). QMEANDisCo-distance constraints applied on model quality estimation. *Bioinformatics (Oxford, England)*, *36*(6), 1765–1771. https://doi.org/10.1093/bioinformatics/btz828

Unal, E., Karakaya, A. A., Beştaş, A., Yıldırım, R., Taş, F. F., Onay, H., Özkınay, F., & Haspolat, Y. K. (2021). Identification of four novel variant in the AMHR2 gene in six unrelated Turkish families. *Journal of Endocrinological Investigation*, *44*(6), 1301–1307. https://doi.org/10.1007/s40618-020-01437-9

van der Zwan, Y. G., Brüggenwirth, H. T., Drop, S. L. S., Wolffenbuttel, K. P., Madern, G. C., Looijenga, L. H. J., & Visser, J. A. (2012). A novel AMH missense mutation in a patient with persistent Müllerian duct syndrome. *Sexual Development*, *6*(6), 279–283. https://doi.org/10.1159/000339704

Waterhouse, A., Bertoni, M., Bienert, S., Studer, G., Tauriello, G., Gumienny, R., Heer, F. T., de Beer, T. A. P., Rempfer, C., Bordoli, L., Lepore, R., & Schwede, T. (2018). SWISS-MODEL: Homology modelling of protein structures and complexes. *Nucleic Acids Research*, *46*(W1), W296–W303. https://doi.org/10.1093/nar/gky427

Weiss, E. B., Kiefer, J. H., Rowlatt, U. F., & Rosenthal, I. M. (1978). Persistent Müllerian duct syndrome in male identical twins. *Pediatrics*, *61*(5), 797–800.

Yu, J., Wang, L., Ma, S., & Li, Z. (2020). Detection and treatment of persistent Mullerian duct syndrome with transverse testicular ectopia. *Urology*, *140*, e4–e5. https://doi.org/10.1016/j.urology.2020.03.014

SUPPORTING INFORMATION

Additional supporting information may be found in the online version of the article at the publisher's website.

How to cite this article: Chen, H., Lin, P., Yuan, X., & Chen, R. (2022). Two novel *AMHR2* gene variants in monozygotic twins with persistent Müllerian duct syndrome: A case report and functional study. *Molecular Genetics & Genomic Medicine*, *10*, e1999. https://doi.org/10.1002/mgg3.1999